8758–8773 *Nucleic Acids Research, 2023, Vol. 51, No. 16* *Published online 23 June 2023*
https://doi.org/10.1093/nar/gkad530

Surveillance of 3′ mRNA cleavage during transcription termination requires CF IB/Hrp1

Jing Li[1,†], Luisa Querl[1,†], Ivo Coban[1], Gabriela Salinas[2] and Heike Krebber[1,*]

[1]Abteilung für Molekulare Genetik, Institut für Mikrobiologie und Genetik, Göttinger Zentrum für Molekulare Biowissenschaften (GZMB), Georg-August Universität Göttingen, D-37075 Göttingen, Germany and
[2]NGS-Serviceeinrichtung für Integrative Genomik (NIG), Institut für Humangenetik, Universitätsmedizin Göttingen, D-37075 Göttingen, Germany

Received September 30, 2022; Revised May 31, 2023; Editorial Decision June 01, 2023; Accepted June 07, 2023

ABSTRACT

CF IB/Hrp1 is part of the cleavage and polyadenylation factor (CPF) and cleavage factor (CF) complex (CPF–CF), which is responsible for 3′ cleavage and maturation of pre-mRNAs. Although Hrp1 supports this process, its presence is not essential for the cleavage event. Here, we show that the main function of Hrp1 in the CPF–CF complex is the nuclear mRNA quality control of proper 3′ cleavage. As such, Hrp1 acts as a nuclear mRNA retention factor that hinders transcripts from leaving the nucleus until processing is completed. Only after proper 3′ cleavage, which is sensed through contacting Rna14, Hrp1 recruits the export receptor Mex67, allowing nuclear export. Consequently, its absence results in the leakage of elongated mRNAs into the cytoplasm. If cleavage is defective, the presence of Hrp1 on the mRNA retains these elongated transcripts until they are eliminated by the nuclear exosome. Together, we identify Hrp1 as the key quality control factor for 3′ cleavage.

GRAPHICAL ABSTRACT

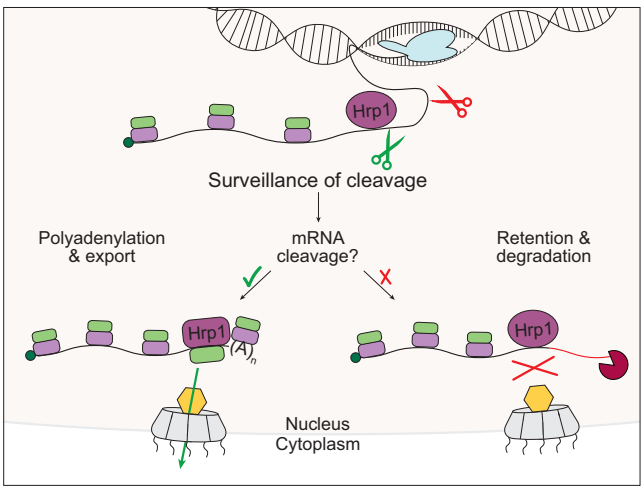

INTRODUCTION

Eukaryotic transcripts are synthesized as precursor mRNAs by RNA polymerase II (RNAP II) and undergo different processing events, such as 5′ capping, splicing and 3′-polyadenylation, before they are exported into the cytoplasm where they are translated as mature mRNAs (1). Processing is monitored, and defective RNAs are eliminated from cells to ensure highly efficient and correct gene expression. In *Saccharomyces cerevisiae,* mRNA surveillance includes the four guard proteins Npl3, Gbp2, Hrb1 and Nab2, which retain transcripts in the nucleus until maturation is completed (2). All guard proteins have in common that (i) their overexpression is toxic and causes mRNA export defects, (ii) they interact with the mRNA export receptor heterodimer Mex67–Mtr2 and (iii) they interact with the nuclear gatekeeper Mlp1 and with the RNA degradation machinery (2–5). When overexpressed, these RNA-binding proteins bind excessively to nuclear transcripts, causing their nuclear retention. Consequently, the lack of any guard

*To whom correspondence should be addressed. Tel: +49 551 39 23801; Fax: +49 551 39 23805; Email: heike.krebber@biologie.uni-goettingen.de
†The authors wish it to be known that, in their opinion, the first two authors should be regarded as Joint First Authors.

protein results in the leakage of faulty transcripts into the cytoplasm (2,3). On correctly processed mRNAs, the guard proteins recruit the export receptor heterodimer Mex67–Mtr2 (TAP–p15 in human) (6). This enables transit through the nuclear pore complex (NPC). Whether an mRNA can indeed pass through the NPC is finally controlled by the nuclear basket protein Mlp1. Mlp1 supports a fast passage of transcripts on which all guard proteins are properly covered with Mex67 and delays passage if the Mex67 coverage is less complete and the ribonucleoparticle differs from the norm (2–4,7,8). This nuclear quality control system ensures the efficient elimination of faulty transcripts from the cell by the 5′ to 3′ acting exonuclease complex Rat1–Rai1, and the nuclear Rrp6-containing exosome that degrades the RNA from its 3′ end (9,10). The exosome is guided to faulty RNAs by assisting complexes, such as the TRAMP (Trf4/5, Air1/2, Mtr4 polyadenylation) complex that marks faulty RNAs with a short oligo(A) tail (11–15).

The different guard proteins function at different stages of pre-mRNA maturation. Npl3 is a quality control factor for proper 5′ capping (16). Its interaction with the cap-binding complex (CBC) is the signal for correct 5′ capping and a prerequisite for Mex67 recruitment, which in turn promotes downstream processing events, such as splicing (17). In cases where the 5′ capping has failed and the CBC is not attached, Npl3 recruits the Rat1–Rai1 complex instead of Mex67, which initiates the 5′ to 3′ degradation of the faulty mRNA (16).

Gbp2 and Hrb1 are preferentially loaded onto transcripts that undergo splicing and interact with the late splicing machinery. Their deletion leads to the leakage of intron-containing pre-mRNAs into the cytoplasm. Therefore, a quality control function for Gbp2 and Hrb1 has been suggested for proper intron excision (2). Interestingly, their quality control function continues in the cytoplasm on spliced transcripts, where they participate in nonsense-mediated decay (NMD) (18). Gbp2 and Hrb1 connect the ends of the transcript with the NMD factor Upf1 that stalls the ribosome on a premature termination codon (PTC) and support translational repression and recruitment of the degradation machinery to the faulty transcript. At the 5′ end they load the decapping factors Dcp1 and Dcp2, and at the 3′ end they recruit Ski2, which in turn captures the exosome for degradation (18). In this way, Gbp2 and Hrb1 connect the nuclear quality control with the cytoplasmic NMD and provide a comprehensive surveillance system for mRNA splicing.

Nab2 binds to transcripts close to the polyadenylation site (19) and has been shown to control the length and quality of 3′ tails (20). Furthermore, it interacts with Mex67, Mlp1 and the nuclear exosome, which is characteristic for nuclear surveillance factors (7,20). Most importantly, its deletion leads to the leakage of faulty mRNAs into the cytoplasm (3).

Thus, a guard protein has been discovered for every processing step, except for 3′ cleavage. One possible candidate to fill in this gap is CF IB/Hrp1/Nab4. Its protein sequence is remarkably similar to those of the guard proteins. It contains two RNA recognition motifs (RRMs), important for RNA binding, and a C-terminal arginine–glycine–glycine (RGG) domain, important for protein–protein interactions and nucleo-cytoplasmic shuttling. In analogy to the other guard proteins, Hrp1 is loaded onto the mRNA in the nucleus and shuttles with the transcript into the cytoplasm. It is part of the multisubunit cleavage and polyadenylation factor (CPF) and cleavage factor (CF) complex important for 3′ end cleavage and release of the pre-mRNA from RNAP II (21,22). The CPF is composed of 15 proteins, which include an endonuclease for RNA cleavage, a poly(A) polymerase for tailing and phosphatases for transcription and 3′ end processing regulation (23). The CF complex is important for tethering the whole CPF–CF complex to the mRNA via binding of the A-rich positioning element (PE) and the UAUAUA-comprising efficiency element (EE) upstream of the cleavage site. The CF complex is divided into CF IA, composed of Rna15 that binds the PE, its interacting protein Rna14 as well as Clp1 and Pcf11, and the CF IB complex, which solely contains Hrp1 that binds to the EE (24–29). The interaction of Hrp1 with Rna14 has been suggested to stabilize the CF I contact with the PE (30). Remarkably, neither Hrp1, the EE nor the PE are essential for cleavage *in vitro* (31,32), suggesting that Hrp1 is not a bona fide cleavage factor. However, it supports the stabilization of the complex, and thus cleavage at this particular site of the RNA (32). Moreover, Hrp1 is the only protein of the CPF–CF complex that shuttles with the mRNA into the cytoplasm (25,33,34).

A second function for Hrp1 has been reported in NMD. It binds a degenerate downstream sequence element (DSE) that is located 3′ of an mRNA PTC and activates NMD through interaction with Upf1 (35). Mutations in *HRP1* have been shown to stabilize nonsense-containing transcripts without affecting the wild-type construct. This reveals interesting similarities with Gbp2 and Hrb1, which were shown to continue their guarding function in the cytoplasm on spliced transcripts in NMD (18). In this way, Gbp2 and Hrb1 link the nuclear and cytoplasmic quality control and have led us to consider that Hrp1 might also function in nuclear quality control. Our experiments show that Hrp1, analogous to the other guard proteins, contacts Mex67 and Mlp1 to support the export of correctly cleaved transcripts. Its overexpression retains mRNAs in the nucleus and its depletion from pre-mRNAs results in the leakage of improperly cleaved transcripts into the cytoplasm. Recognition of correct cleavage occurs via interaction of Hrp1 with Rna14, which ultimately results in the recruitment of the export receptor Mex67–Mtr2. These findings support a novel function for Hrp1 as an mRNA guard protein for 3′ end cleavage.

MATERIALS AND METHODS

Yeast strains and plasmids

All yeast strains used in this study are included in Supplementary Table S1. Yeast cells with metabolic auxotrophies to certain amino acids (L-adenine, L-histidine, L-leucine, L-lysine and L-tryptophan) or uracil were either grown in YPD full medium or in selective medium, depending on whether they contained a plasmid with the marker gene that granted prototrophy for auxotrophic growth. To induce a gene under the *GAL1* promoter for overexpression, galactose was added for 2–3 h. To repress gene expression under

the *GAL1* promoter, galactose was replaced with glucose for the indicated times. Cells were cultivated at 25°C, but, in the case of temperature-sensitive mutants being used, all strains were shifted to the restrictive temperature for the indicated time. Cells were harvested at the logarithmic phase (1–3 × 10^7 cells/ml). To create double or triple mutants, parental haploid strains with opposite mating types were crossed, and the diploid cells were sporulated in a medium with a low nutrient level. Following tetrad dissection and selective plate screening, polymerase chain reaction (PCR) was carried out to confirm positive spores with genetic markers and gene deletions. Supplementary Table S2 lists all the plasmids used in this study. Plasmids were cloned via either Gibson assembly or restriction-free cloning (36). The lithium acetate method was used to transform yeast strains with plasmids (37). Supplementary Tables S3, S4 and S5 list all the oligonucleotides used for cloning, quantitative PCR (qPCR) and analytical PCR in this study, respectively.

Yeast growth test

Overnight pre-cultures of yeast strains were diluted in sterile H_2O and counted under a light microscope. For each strain, 10-fold serial dilutions of 10^7, 10^6, 10^5, 10^4 and 10^3 cells/ml were made, and cells were spotted onto agar plates. Plates were scanned after incubation at different temperatures (16, 25, 30, 35 and 37°C) for 2–3 days. The intensity and size of yeast colonies on plates were compared to analyze the growth of yeast cells; therefore, genetic interactions could be determined.

Co-immunoprecipitation experiments

The co-immunoprecipitation (co-IP) experiments were carried out as described earlier (3). Following harvest, cells were lysed in PBSKMT buffer [1× phosphate-buffered saline (PBS) pH 7.5, 3 mM KCl, 2.5 mM $MgCl_2$, 0.5% Triton X-100 and a protease inhibitor] with glass beads and a FastPrep cell homogenizer (3 × 30 s, 5 min on ice in between). Green fluorescent protein (GFP)-trap or MYC-trap beads were used to pull-down GFP-tagged or MYC-tagged proteins. After washing, both lysates and eluates were mixed with 2× sodium dodecylsulfate (SDS) sample buffer and denatured at 95°C for 6–8 min. All samples were loaded onto a 10% SDS–polyacrylamide gel and the target proteins were analyzed via western blot with corresponding antibodies.

Combined *in vivo*/*in vitro* binding study

For Figure 1H, *in vivo* and *in vitro* protein binding were combined. The recombinant Mex67–Mtr2 was expressed as described earlier (38), while MYC-tagged Hrp1 was expressed from yeast *in vivo* and precipitated with MYC-trap beads as described for the co-immunoprecipitation experiments. Beads were washed five times with PBSKMT buffer and a third of the beads were collected. The remaining beads were incubated with *in vitro* lysis buffer [50 mM Tris–HCl pH 7.5, 150 mM NaCl, 2 mM $MgCl_2$, 5% (v/v) glycerol, 1 mM dithiothreitol (DTT), 0.2% (v/v) NP-40 and a protease inhibitor (Roche)] at 8°C for 20 min and afterwards washed six times with *in vitro* lysis buffer. From the remaining beads, half were again collected. Recombinant protein was added to the residual beads and the samples were incubated at 8°C for 1.5 h. Finally, the beads were washed six times with *in vitro* lysis buffer and all samples were submitted to SDS–polyacrylamide gel electrophoresis (PAGE) and western blotting.

Western blot

All co-IP experiments that are shown in any one figure stem from the same gel. Nitrocellulose membranes were cut horizontally to be able to probe with different antibodies simultaneously, but were pieced back together before detection. An example of a full blot is shown in Supplementary Fig. S1E. All primary antibodies used in this study are listed in Supplementary Table S6. Secondary anti-mouse or anti-rabbit IgG–horseradish peroxidase (HRP; Dianova) were diluted 1:10 000 and detected with WesternBright Quantum HRP Substrate (Advansta). Signals were detected with the FUSION FX chemiluminescence detection system (Peqlab). Signal intensity was quantified using the Bio1D software (Peqlab).

RNA co-immunoprecipitation experiments

RNA co-IP (RIP) assays were performed to analyze the RNA binding of target proteins as described earlier (3). Cells were lysed in RIP buffer [25 mM Tris–HCl pH 7.5, 2 mM $MgCl_2$, 150 mM NaCl, 0.5 mM DTT, 0.2% Triton X-100, protease inhibitor, 0.2 mM phenylmethylsulfonyl fluoride (PMSF) and 0.02 U/ml Ribolock] with glass beads utilizing a FastPrep cell homogenizer. GFP-trap beads were used to pull-down GFP- or MYC-tagged proteins. Samples were split after washing. One part was loaded on an SDS gel and checked for pulldown on a western blot, while the other part was used for RNA isolation and RNA binding analyses by qPCR. RNAs from both the lysate and the eluate were extracted with Trizol and purified with phenol–chloroform. cDNAs were synthesized with the FastGene Scriptase II Kit (NIPPON Genetics) by using random hexamer primers.

Fluorescence *in situ* hybridization (FISH)

FISH experiments were performed as described earlier (3). A Cy3-labeled oligo $d(T)_{50}$ probe was used to detect mRNAs with a poly(A) tail in yeast cells. Following a shift to the non-permissive temperature, cells were fixed by adding 37% formaldehyde to a final concentration of 4% for 45 min and afterwards harvested. Cells were washed with P solution (1.2 M sorbitol, 0.1 M phosphate buffer pH 6.5) and treated with DTT (10 mM) for 10 min. Subsequently, cells were digested with zymolyase (10 mg/ml) for 10–30 min and applied onto slides coated with poly-L-lysine for 30–60 min. To enable the probe to penetrate the nuclear envelope, cells were treated with 0.5% Triton X-100 in P solution for 10 min. To reduce unspecific staining in the background, the pre-hybridization buffer [50% deionized formamide, 5× SSC, 2.5 mM EDTA pH 8.0, 0.1% Tween-20, 5× Denhardt's, 50 μg/ml heparin and diethylpyrocarbonate-treated water (DEPC H_2O)] was added onto the slide in a humidified chamber at 37°C for 30–60 min. The Cy3-labeled oligo $d(T)_{50}$ probe was diluted 1:200 in the pre-hybridization buffer and applied to cells on the slide for

in situ hybridization overnight at 37°C. Cells were washed with 2× SSC (0.3 mM NaCl, 30 mM sodium citrate, pH 7), 1× SSC and 0.5× SSC for 1 h, respectively, and incubated with 4′,6-diamidino-2-phenylindole (DAPI; 1:10 000) in PBS for nuclear staining. Following 3–5 washes with PBS, the slide was dried, coated with mounting medium (2% *n*-propyl gallate, 80% glycerol, 20% PBS pH 8) and sealed. The DFC360 FX camera of the Leica DMI6000B fluorescence microscope was used to detect cell fluorescence. The LAS AF1.6.2 software was used to capture pictures under the microscope.

GFP microscopy

GFP microscopy was conducted as described earlier (16). Cells were grown to log phase and shifted for 1 h at 37°C. For nuclear staining, DAPI was used in a 1:5000 dilution in Aby Wash 2.

Cell fractionation

The cell fractionation assay was carried out to examine leakage of 3′-extended faulty mRNAs in the cytosol as described earlier (39). Following harvest, the logarithmic cells were washed with H_2O and YPD/1 M sorbitol/2 mM DTT, respectively, and then digested with zymolyase in YPD/1 M sorbitol/1 mM DTT for 10–30 min to obtain spheroplasts. After 30 min of recovery in YPD/1 M sorbitol at 25°C, cells were shifted to 37°C for 3 h to induce the mutant phenotype. Then, cells were lysed and the cytosolic fraction was obtained in the supernatant of the Ficoll density gradient after centrifugation. Antibodies of the nuclear proteins Nop1 or Yra1 and the glycolytic enzyme Zwf1 were used to confirm the successful separation of the cytosolic fraction on the western blot. Total RNA was isolated from both the lysate and the cytosolic fraction with the NucleoSpin RNA kit (MACHEREY-NAGEL). cDNAs were synthesized with the FastGene Scriptase II Kit (NIPPON Genetics) by using random hexamer primers. Leakage of readthrough mRNAs was analyzed via qPCR with primers flanking the cleavage site.

RNA-sequencing

RNA samples obtained by cytoplasmic fractionation were sequenced at the NGS-Integrative Genomics Core Unit, University Medical Center Göttingen. RNA integrity and subsequent library quality were determined using the Fragment Analyzer. Sequencing was carried out with the NovaSeq6000 (PE 100 cycles; 30 Mio reads/sample). A modified TruSeq Stranded Total RNA Library Prep (Cat. No. 20020596) was used, starting with 200 ng of total RNA. The resulting fastq files were mapped to the *S. cerevisiae* genome sacCer3 with Hisat2 (40). Hisat2 was run twice to generate strand-specific bam files for downstream applications, once skipping the reverse strand and once the forward strand. Next, the fragment coverage of genomic regions was calculated with deeptools2 and a bin size of 1 (41). Either the stop codon (1) or the annotated transcript ends (2) of Tudek *et al*. (42) were used as the reference point ± 200 nucleotides. For coding sequence (CDS) coverage, every CDS was scaled to 100 nucleotides (3). The mean of every position between transcripts of (1) and (2) was calculated and divided by the mean coverage of the CDS (3). Each position was again normalized to the wild type and the graph was plotted using GraphPad Prism.

mRNA isolation

Poly(A)$^+$ mRNAs were isolated from total RNAs using the Dynabeads™ mRNA Purification Kit (Invitrogen). Total RNAs were extracted with the NucleoSpin RNA kit (MACHEREY-NAGEL).

qPCR analysis of 3′-extended mRNAs

Cells were harvested mid log phase after a shift to 37°C for 3 h. Cell pellets were lysed as described for the RIP experiments. DNA was digested by treatment with rDNase for 1 h at 25°C. RNA extraction and qPCR analysis were conducted in the same way as described for the RIP experiments.

Quantification

All experiments shown in this work were carried out at least three times independently. Error bars represent the standard deviation (SD). The *P*-values that were determined by *t*-test (two tails, heteroscedastic type) of two unpaired arrays are indicated as follows: ***$P < 0.001$, **$P < 0.01$, *$P < 0.05$.

RESULTS

Hrp1 interacts with Mex67 and Mlp1, and can retain mRNAs in the nucleus

So far, guard proteins have been identified to monitor every mRNA processing step except 3′ cleavage (Figure 1A). We suspected that Hrp1/CF IB might be responsible for the quality control of this cleavage, as it is part of the 3′ CPF–CF complex and shows high homology to the other guard proteins (Figure 1B). We investigated whether Hrp1 would also behave like them. First, we overexpressed the protein on a plasmid from a strong galactose promoter and visualized the growth of a wild-type strain in the presence and the absence of high copy *HRP1*. We found that the overexpression of *HRP1* is indeed toxic to cells, as shown by drop dilution assays (Figure 1C). Most importantly, the excess of Hrp1 caused strong mRNA export defects visible in FISH experiments with a Cy3-labeled oligo $d(T)_{50}$ probe (Figure 1D), suggesting that Hrp1 can retain mRNAs in the nucleus. Since the export defect could not be detected in every cell, we examined the expression of Hrp1 via GFP microscopy (Supplementary Figure S1A) and could confirm that the uneven retention is most probably due to an uneven expression of *HRP1*.

In co-IP experiments, we found interactions of Hrp1 with both the export receptor Mex67 and the gatekeeper Mlp1 (Figure 1E, F; Supplementary Fig. S1D). Both interactions were RNase insensitive, suggesting that the proteins are in the same complex. Furthermore, mutant *hrp1* exhibited genetic interactions with mutants of *MEX67* and *MLP1*, since the double mutants *hrp1-1 mex67-5* and *hrp1-1 mlp1Δ* had

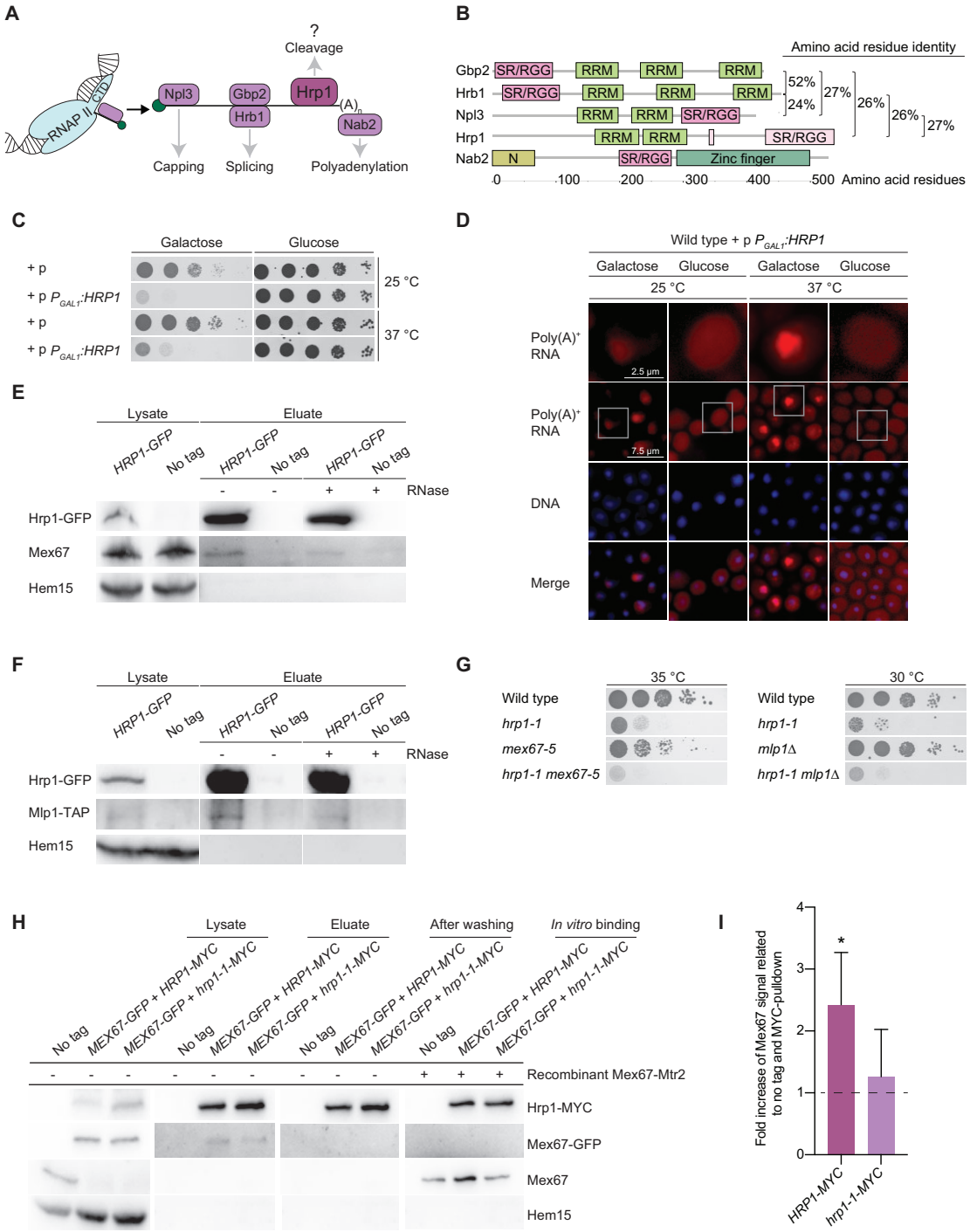

Figure 1. Hrp1 shares features with the other guard proteins. (**A**) Scheme of nuclear mRNA quality control factors that monitor different pre-mRNA processing steps. Hrp1 is a potential guard protein for 3′ cleavage. (**B**) The shuttling RNA-binding protein Hrp1 shares significant similarities with the known guard proteins. The amino acid sequences of the depicted proteins were aligned, and the motifs as well as the sequence identity are shown. (**C**) Overexpression of *HRP1* is toxic to cells. The indicated strains were spotted in 10-fold serial dilution onto agar plates. The growth is shown at the indicated temperatures after 2 days of incubation; $n = 3$. (**D**) Overexpression of Hrp1 leads to nuclear mRNA accumulation. FISH experiments were carried out with a Cy3-labeled oligo $d(T)_{50}$ probe. The DNA was stained with DAPI. The signal intensity differs because of the uneven expression of Hrp1–GFP from the *GAL1* promoter; $n = 3$. (**E**) Hrp1 interacts with Mex67. A western blot of co-immunoprecipitated Mex67 with GFP-tagged Hrp1 is shown. The mitochondrial protein Hem15 served as a negative control; $n = 3$. (**F**) Hrp1 interacts with Mlp1. A western blot of co-immunoprecipitated TAP-tagged Mlp1 with Hrp1–GFP is shown; $n = 3$. (**G**) *HRP1* genetically interacts with *MEX67* and *MLP1*. Ten-fold serial dilutions of the indicated strains grown on selective agar plates are shown after 2 days of growth at the indicated temperatures; $n = 3$. (**H**) Hrp1 directly binds Mex67. MYC-tagged Hrp1 was precipitated *in vivo* and all interacting proteins were removed by rigorous washing. Purified Mex67 was added *in vitro* and binding was analyzed via western blot utilizing a polyclonal direct Mex67 antibody. As shown in Supplementary Fig. S1E, the membrane was cut prior to probing; $n = 5$. (**I**) Quantification of the Mex67 signal from (H). Since unspecific binding of Mex67 to the MYC-trap beads could not be prohibited completely, the intensity of the Mex67 signal was measured and related to the no tag control and MYC pulldown; $n = 5$.

stronger growth defects at the indicated temperatures than the single mutants (Figure 1G; Supplementary Fig. S1B, C). To ensure that Hrp1 is able to directly bind Mex67 and does not simply interact with the export receptor due to being present in the same complex, we precipitated Hrp1 expressed from yeast cells *in vivo* and analyzed the binding of purified Mex67–Mtr2 expressed from *Escherichia coli in vitro* (Figure 1H, I). Reassuringly, binding between Hrp1 and Mex67 was detected. However, this interaction was strongly decreased upon the mutation of Hrp1, indicating that hrp1-1, which had been identified earlier (32), has defects either in binding to Mex67 or in an upstream process that prevents Mex67 recruitment. Combined, these findings show that Hrp1 behaves very similarly to the other guard proteins and indicates a potential involvement of this protein in the nuclear mRNA quality control pathway.

Mutant *hrp1-1* has lost its RNA binding specificity

To analyze whether Hrp1 can actively retain faulty mRNAs in the nucleus, we wanted to conduct a leakage assay that we have developed earlier (2,3). In this assay, we use a mutant of the nuclear exosome, *rrp6Δ*, to visibly accumulate mostly faulty mRNAs in the nucleus. In the presence of the guard proteins, the defective RNA is retained in the nucleus and awaits its degradation, which is slowed in *rrp6Δ*, resulting in the visible nuclear accumulation of the mostly faulty mRNAs. However, the simultaneous deletion of any guard protein leads to the leakage of the faulty transcripts into the cytoplasm (2,3). Therefore, we wanted to carry out a similar experiment with Hrp1. For this purpose, we chose two approaches: First, we depleted Hrp1 from cells through a regulable galactose-inducible promoter ('conditional' *hrp1Δ*) as reported earlier (43), and, secondly, we used a mutant termed *hrp1-1* that was identified as temperature sensitive (32). It was shown that *hrp1-1* grows well at 25°C but dies at 37°C; however, further characterization was lacking. Therefore, we first sequenced the mutant and found it to contain nine amino acid exchanges, four of which were clustered in the RRMs, suggesting that the mutant protein might have an altered RNA binding behavior if not degraded (Figure 2A). Hence, we first analyzed its stability on western blots and found it not to be affected (Figure 2B). Subsequently, we addressed whether it had lost its RNA binding activity. For this purpose, we carried out RIP assays and could show that this was not the case. On the contrary, mutant *hrp1-1* bound almost four times more RNA than the wild-type protein (Figure 2C, D). Strikingly, however, further analysis of this mutant revealed that the hrp1-1 protein exhibits an altered RNA binding specificity. Known targets, which contain the EE sequence UAUAUA (*MRP2*, *MEX67*, *ACT1*, *MRP2* and *RAI1*) or one of its variants (*ADH1* and *CYC1*) to which this RNA-binding protein usually binds, show reduced binding in RIP assays, while the binding to targets without the EE, such as rRNAs, was increased (Figure 2E). Thus, phenotypically, the interaction of hrp1-1 with its target mRNAs appears to be reduced and the protein may further be missing in the termination reaction. In this way, it might have a very similar phenotype to the down-regulation of the wild-type gene. Most importantly, both the conditional knockout that shows a protein depletion after 1–3 h of incubation in glucose, and the *hrp1-1* mutant that was shifted to 37°C for 3 h, showed no mRNA accumulation in the nucleus (Figure 2F, G). For these reasons, we were able to carry out the leakage assay with both strains.

Hrp1 retains cleavage-defective transcripts in the nucleus

The depletion of hrp1-1 from its natural EE-containing mRNA targets allowed us to perform the leakage assay with this mutant. Additionally, we investigated mRNA leakage in the *hrp1Δ* strain. If Hrp1 would indeed function as an mRNA surveillance factor, its absence should result in the leakage of faulty mRNAs into the cytoplasm. For visualization of this potential loss of function, we crossed P_{GAL1}*:HRP1* and the *hrp1-1* mutant strain with the nuclear exosome mutant strain *rrp6Δ*, in which defective RNAs visibly accumulate in the nucleus, and analyzed the growth of the double mutants. For *hrp1Δ*, growth on glucose-containing plates was impossible at all tested temperatures (Figure 3A), since *HRP1* is essential and its expression from the *GAL1* promoter is suppressed in the presence of glucose. At 37°C, the growth of *hrp1Δ* on galactose-containing plates was also restricted, probably due to a stronger toxicity resulting from *HRP1* overexpression. This differs from the experiment shown in Figure 1C, which was carried out in the presence of the endogenous *HRP1*, while in Figure 3A the galactose-inducible *HRP1* is the only copy. Interestingly, P_{GAL1}*:HRP1 rrp6Δ* exhibits a synthetic growth defect which may be due to the fact that *HRP1* expression appears to be lower in this strain (Figure 2F). In contrast, while *hrp1-1* grows well at 25°C, growth of the double mutant *hrp1-1 rrp6Δ* was slightly affected, which uncovers a genetic interaction (Figure 3B). At 37°C, both strains, the *hrp1* single mutant and the double mutant strain, are dead. This growth defect was partially rescued by ectopically expressed wild-type *HRP1*. Importantly, FISH experiments with a Cy3-labeled oligo $d(T)_{50}$ probe, that clearly detected a nuclear accumulation of the faulty mRNA in *rrp6Δ*, revealed leakage of these faulty transcripts into the cytoplasm in *rrp6Δ*P_{GAL1}*:HRP1* and in *rrp6Δ hrp1-1* double mutants (Figure 3C). This effect was reversed through ectopically expressing wild-type *HRP1*, confirming that the effect is due to non-functional Hrp1.

As Hrp1 was identified to be part of the CPF–CF complex, we suspected that it might monitor the 3′ end cleavage of pre-mRNAs that contain an EE. Thus, we used a cleavage-defective mutant of a component of this complex, *cft2-1*, crossed it either with the conditional *hrp1Δ* or with the *hrp1-1* strain and analyzed the growth of these strains. The *hrp1-1 cft2-1* double mutant shows a genetic interaction (Figure 3D; Supplementary Fig. S2B). However, as slow growth was possible, we repeated the leakage assay for cleavage-defective transcripts. Due to the cleavage defect, faulty mRNAs accumulate in the nuclei of *cft2-1* mutants as shown in FISH experiments (Figure 3E). However, when combined with *hrp1Δ* or *hrp1-1*, the nuclear retention of the faulty mRNA was released (Figure 3E). Because the faulty mRNAs are rapidly degraded in *cft2-1*, as this is in the background of an intact quality control system, we

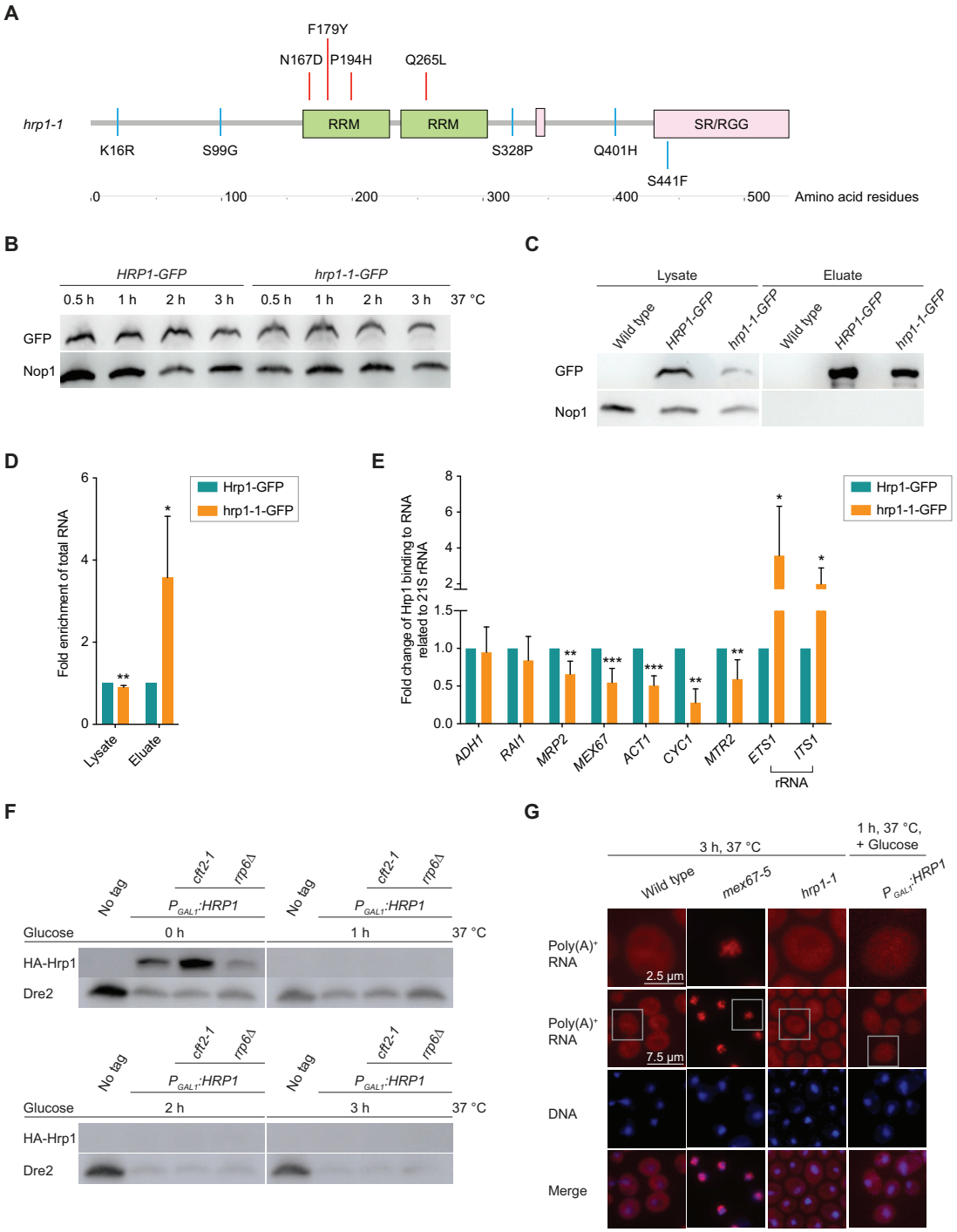

Figure 2. Characterization of *hrp1-1* and the conditional knockout strain of *HRP1*. (**A**) Amino acid substitutions in the mutant *hrp1-1* cluster in the RRMs. The red bars indicate the mutations in the RRMs and the blue bars show additional alterations in the open reading frame. (B) The hrp1-1 protein has no decreased stability. Western blots show the hrp1-1 expression after a temperature shift to 37°C. Nop1 served as a loading control; $n = 4$. (**C**) hrp1-1–GFP is enriched after pulldown. An example western blot for GFP-tagged Hrp1 or hrp1-1 pulldown is shown for the indicated strains. Protein amounts were measured via Image J. Nop1 served as a negative control; $n = 6$. (**D**) The mutated hrp1-1 protein shows an increased binding to RNA. Wild-type and *hrp1-1* cells were grown to log phase before they were shifted to 37°C for 3 h. Both GFP-tagged Hrp1 and hrp1-1 were precipitated from the lysates, and the co-precipitated RNA was purified and measured at OD_{260}. The signal intensity of each pulldown (such as shown in C) was related to that of the no tag control. Thereafter, the fold enrichment of the RNA precipitated by hrp1-1 was obtained via relating it to that of Hrp1; $n = 6$. (**E**) hrp1-1 has lost its binding specificity. The RNAs obtained in the pulldown experiments (shown in C and D) were analyzed for the indicated specific mRNA targets and two unspecific rRNA targets by qPCR; $n \geq 6$. (**F**) Hrp1 is depleted in the conditional knockout strain P_{GAL1}*:HRP1* upon addition of glucose. A western blot analysis revealed that Hrp1 expression is undetectable in P_{GAL1}*:HRP1* grown with glucose at 37°C in the indicated strains; $n = 3$. (**G**) Both *hrp1-1* after temperature shift and P_{GAL1}*:HRP1* under repressing conditions have no mRNA export defect. The indicated strains were grown to log phase and shifted to 37°C for 3 h or 1 h. The poly(A)$^+$ RNA was detected with a Cy3-labeled oligo d(T)$_{50}$ probe. Nuclear retention of poly(A)$^+$ RNA in *mex67-5* served as a positive control; $n = 3$.

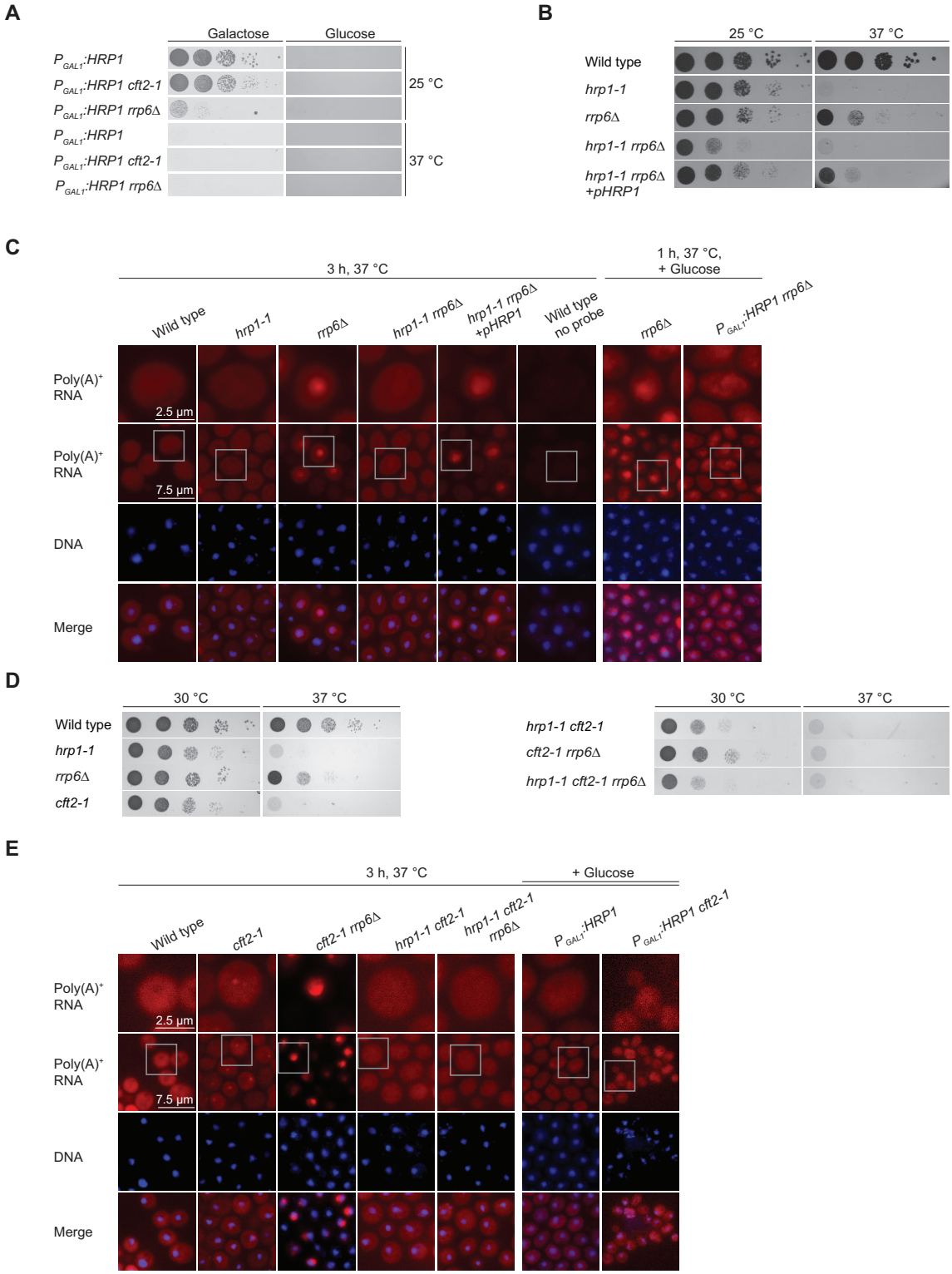

Figure 3. Mutations in *HRP1* result in the leakage of 3′-extended faulty mRNAs into the cytoplasm. (**A**) Glucose represses the growth of P_{GAL1}:*HRP1*. Ten-fold serial dilutions of the indicated strains were spotted onto agar plates with either glucose or galactose, and incubated for 2 days; $n = 3$. (**B**) The double mutant strain *hrp1-1 rrp6Δ* is viable at 25°C but grows more slowly than the single mutants. Ten-fold serial dilutions of the indicated strains were spotted onto agar plates that were incubated for 2 days; $n = 3$. (**C**) Faulty mRNA is not retained in *rrp6Δ* when *HRP1* is mutated or conditionally knocked out. A leakage assay is shown for the indicated strains after the temperature shift or after down-regulation of *HRP1* expressed from the galactose-inducible promoter. The FISH experiment was carried out with a Cy3-labeled oligo (d)T_{50} probe targeting mRNAs with a poly(A) tail. The nucleus was stained with DAPI; $n = 3$. (**D**) The double mutant strain *hrp1-1 cft2-1* is viable at 30°C but grows more slowly than the single mutants. Ten-fold serial dilutions are shown on plates that were incubated for 2 days; $n = 3$. (**E**) Faulty mRNA is not retained in *cft2-1* when *HRP1* is mutated. A leakage assay as described in (D) is shown for the indicated strains; $n = 3$.

also generated a *cft2-1 rrp6Δ* double mutant that, although slow growing, was viable (Figure 3D). In the double mutant *rrp6Δ cft2-1*, the nuclear accumulation of the cleavage-defective pre-mRNAs was enhanced, as shown in *in situ* hybridization experiments (Figure 3E). Most importantly, this nuclear signal also disappeared when *HRP1* was mutated or conditionally deleted (Figure 3E). Finally, in order to ensure that Hrp1 is indeed able to affect nuclear processing in all strains, we investigated the localization of mutant and wild-type Hrp1 utilizing GFP microscopy and could show that the localization of the protein is primarily nuclear in all backgrounds (Supplementary Fig. S2A). In order to ensure that the decrease of nuclear signal in the FISH experiments is not simply due to a more efficient degradation in *hrp1-1*, we determined the mRNA levels in the *rat8-2* mRNA export mutant and a *rat8-2 hrp1-1* double mutant, and could show that the mRNA levels did not decrease in the absence of Hrp1 (Supplementary Fig. S2C). These results reveal that the presence of intact Hrp1 is necessary to visibly retain faulty transcripts in the nucleus until they are degraded.

Elongated mRNAs escape nuclear decay in the absence of Hrp1

To verify that faulty mRNAs generated in *cft2-1* are indeed cleavage defective, we utilized primers to amplify potential 3′-extended forms (Figure 4A). The primers were designed to flank the cleavage site and positioned upstream of possible NNS-binding sites. These elongated mRNAs are released from RNAP II downstream of the CPF–CF site, possibly through action of the NNS system, composed of Nrd1, Nab3 and Sen1, which acts as a fail-safe mechanism that directs faulty mRNAs directly into degradation (44–46). NNS sites downstream of the CPF–CF sites are present in basically all mRNAs. To identify how many transcripts were elongated in relation to wild-type cells, we determined the amounts of the elongated transcripts in *cft2-1*, *hrp1-1* and the *hrp1-1 cft2-1* double mutant for four randomly chosen transcripts (*ACT1*, *ADH1*, *MRP2* and *MEX67*). Both single mutants *cft2-1* and *hrp1-1* show an increase of faulty transcripts, with an ∼2.6-fold increase for *hrp1-1* and an even higher amount detected in *cft2-1*, ∼5.2-fold on average (Figure 4B; Supplementary Fig. S3A) (32). Importantly, in the double mutant *hrp1-1 cft2-1*, we detected on average more than an ∼10.4-fold increase of the 3′-extended mRNAs (Figure 4B; Supplementary Fig. S3A), suggesting that more of the faulty mRNAs generated in *cft2-1* might escape the Hrp1-mediated nuclear surveillance and degradation in the nucleus. It is assumed that defective CPF–CF termination leads to the recognition of the downstream NNS-mediated termination site and the subsequent elimination of readthrough mRNAs by the nuclear exosome (44–46). To verify this for our chosen transcripts, we first investigated whether the 3′-extended mRNA would accumulate in an NNS mutant, which was indeed the case (Figure 4C; Supplementary Fig. S3B). Similar to the *hrp1* mutant in the background of *cft2-1,* in which many extended transcripts are generated and escape nuclear elimination, the simultaneous mutation of *NRD1* in *cft2-1* also resulted in an ∼12.1 -fold increase of the faulty transcripts (Figure 4C; Supplementary Fig. S3B) in combination with severe growth defects, visible in a drop dilution assay (Figure 4D). If the degradation machinery is not able to eliminate increased amounts of elongated mRNAs as present in *nrd1-102 cft2-1*, this may imply that the cells are overwhelmed by the presence of faulty transcripts, which leads to the observed growth defect.

To finally bring the nuclear degradation of the faulty transcripts into context with the cytoplasmic leakage, we examined the accumulation of readthrough mRNAs in *cft2-1*, *hrp1-1* and the double mutant *hrp1-1 cft2-1* in the background of *rrp6Δ*. While *rrp6Δ* showed only a slight increase, as did the *hrp1-1 rrp6Δ* double mutant, *cft2-1 rrp6Δ* showed a >20-fold increase (Figure 4E; Supplementary Fig. S3C). These findings show that only a few RNAs are 3′ cleavage defective in *rrp6Δ* and that this is similar in *hrp1-1 rrp6Δ*. This demonstrates that not many transcripts have defects in cleavage under normal conditions and it furthermore supports the fact that Hrp1 is not necessary for the cleavage reaction itself. In *cft2-1,* however, many transcripts are generated that await degradation in the absence of *RRP6*, as we saw a >20-fold increase on average. Interestingly, the situation changes dramatically when *HRP1* is additionally mutated. In the triple mutant *hrp1-1 cft2-1 rrp6Δ*, we found a reduction of the faulty transcripts by half, suggesting that they escape nuclear retention and are instead captured, at least partially, by the cytoplasmic quality control system (Figure 4E; Supplementary Fig. S3C).

To be able to distinguish between their presence in the nucleus and in the cytoplasm, we carried out nucleo-cytoplasmic fractionation experiments (Figure 4F), in which we were able to analyze the cytoplasmic aberrant mRNA content in relation to the total faulty mRNAs in the lysate. Subsequent qPCRs revealed that in the presence of intact Hrp1, these elongated transcripts did not leak into the cytoplasm (Figure 4G; Supplementary Fig. S3D). In contrast, non-functional hrp1-1 led to the leakage of 3′-readthrough mRNAs into the cytoplasm (Figure 4G; Supplementary Fig. S3D). The more of them that were generated, such as in *hrp1-1 cft2-1*, the more were cytoplasmic.

To analyze the situation transcriptome wide, we repeated the nucleo-cytoplasmic fractionation experiment with the wild type and the *hrp1-1* mutant shifted for 3 h to the non-permissive temperature, and found that more transcripts with elongated 3′ ends reached the cytoplasm in the mutant than in wild-type cells (Figure 4H–J). When comparing the read coverage around transcript ends in the cytoplasm normalized to the CDS, we could observe an increase in *hrp1-1* over the wild type that is especially prominent downstream of the annotated transcript ends (peak shift right from main annotated transcript ends) (Figure 4I). A significant number of transcript ends showed a significant increase in the ratio of downstream to upstream read coverage in *hrp1-1* compared with the wild type (Figure 4J). On average, we detected an ∼2-fold increase of the elongated transcripts in the cytoplasm of *hrp1-1* which is contributed to by >60% of all expressed transcripts (Figure 4K, L). These findings confirm Hrp1 as a novel mRNA quality control factor responsible for the retention of cleavage-defective mRNAs in the nucleus.

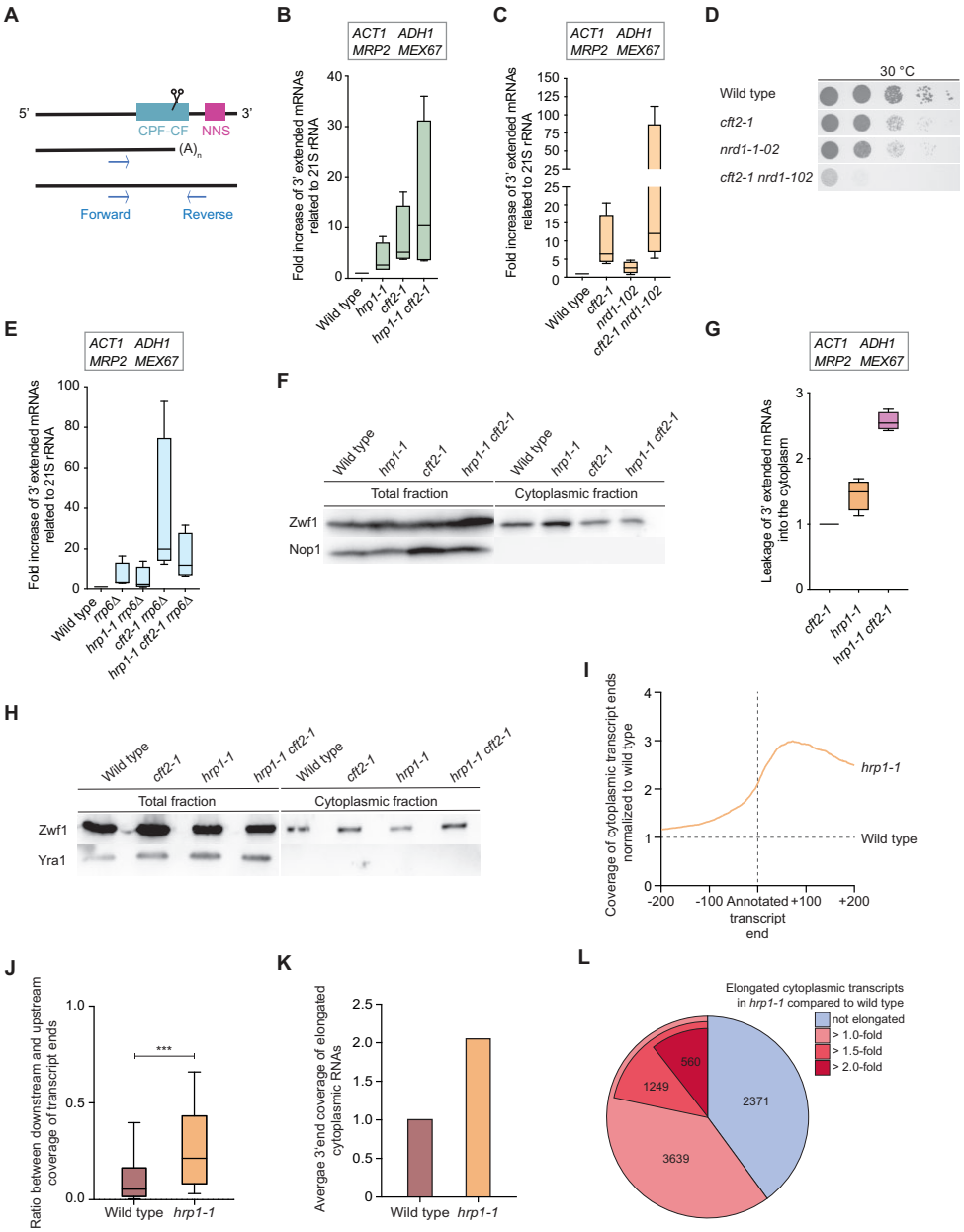

Figure 4. Readthrough mRNAs are retained in the nucleus by Hrp1. (**A**) Primers that flank the cleavage site were designed to detect specific readthrough transcripts. CPF–CF and downstream-located NNS termination sites are indicated. (**B**) Hrp1 is required for the reduction of readthrough transcripts. The cellular content of the 3′-extended mRNAs is shown in the indicated mutants in relation to the wild type. For each strain, the amount of readthrough transcripts of four randomly chosen mRNA targets (*ACT1*, *ADH1*, *MRP2* and *MEX67*) is shown. For each mRNA target, the enrichment was related to the mitochondrial 21S rRNA. The RNAs were isolated from cell lysates of the indicated strains; $n \geq 7$. (**C**) 3′-Extended mRNAs in *cft2-1* are terminated by the NNS pathway. Accumulation of readthrough mRNAs for the indicated strains was detected as described in (B); $n = 4$. (**D**) Genetic interaction between *cft2-1* and the NNS mutant *nrd1-102* is shown in drops from 10-fold serial dilutions of the indicated strains after growth for 2 days; $n = 3$. (**E**) Readthrough transcripts are degraded by the nuclear exosome and escape nuclear degradation when *HRP1* is mutated. The amount of readthrough mRNAs for the indicated strains was detected as described in (B); $n \geq 7$. (F) An example western blot of the cell fractionation experiment used in (G) is shown. The glycolytic enzyme Zwf1 and the nucleolar protein Nop1 were used as cytosolic and nuclear markers, respectively. (**G**) Non-functional hrp1-1 leads to significant leakage of 3′-elongated mRNAs into the cytoplasm of *hrp1-1 cft2-1*. Cells were shifted to 37°C for 3 h and the total and cytoplasmic RNAs were obtained via cytoplasmic fractionation. The leakage was determined by the ratio of faulty mRNAs in the cytoplasm to those in the total lysate. The fold enrichment of each readthrough mRNA target was determined via qPCR in relation to that of the wild type and, subsequently, to *cft2-1*; $n \geq 6$. (**H**) Western blot of the cell fractionation used for RNA-sequencing. Zwf1 was used as a cytosolic marker, while the RNA-binding protein Yra1 was used as a nuclear marker; $n = 1$. (**I**) The leakage of 3′-elongated mRNAs into the cytoplasm is a transcriptome-wide effect in *hrp1-1*. Total RNA-seq was carried out in *hrp1-1* and the wild type. Aligned read coverage at transcript ends (± 200 nt) identified by Tudek *et al.* (42) was calculated via deeptools2; $n = 1$. (**J**) For each transcript, the read coverage at their transcript ends was calculated individually. For that, the region at the annotated transcript ends was divided into an upstream (transcript end –200 nt) and a downstream (transcript end +200 nt) part. The resulting coverage of both areas was put into relation (downstream coverage/upstream coverage); $n = 1$. (**K**) The total read coverage downstream of the annotated transcript ends (+200) was related to the upstream coverage (–200) and normalized to the wild type; $n = 1$. (**L**) The number of elongated transcripts in the cytoplasm was counted and grouped based on their fold increase of read coverage ratio between *hrp1-1* and the wild type calculated in (J); $n = 1$.

Mex67 is not recruited to cleavage-defective mRNAs

To finally show why the cleavage-defective pre-mRNAs are not retained in the nucleus when Hrp1 is missing, and to get some insights into the underlying mechanism, we investigated the binding of the export receptor heterodimer Mex67–Mtr2 to Hrp1 in the cleavage-defective mutant *cft2-1*. Since earlier studies have shown that mRNAs are rapidly degraded in *cft2-1* when shifted to 37°C, we first tested whether readthrough mRNAs generated at 30°C are more stable in this mutant (47). For this purpose, wild-type and *cft2-1* cells were grown to log phase at 30°C. Equal amounts of cells were lysed, and the total RNA as well as the poly(A)$^+$ RNA content were determined to be almost equal (Figure 5A). At this temperature, while an equal Mtr2 pulldown resulted in equal amounts of Mex67 in both strains, an interaction with Hrp1 was only detected in wild-type cells (Figure 5B). Thus, it seems that defects in the cleavage reaction prevent binding between Hrp1 and Mex67, which would inhibit the nuclear export of the bound mRNA. We repeated this pulldown experiment, but this time we used the Hrp1-interacting protein Rna14 as bait. Likewise, we found that both Hrp1 and Mex67 interact with Rna14 in wild-type cells but not in *cft2-1* (Figure 5C). These findings support the idea that controlled Mex67 recruitment by Hrp1 determines nuclear export and that only Rna14-bound Hrp1 can interact with the export receptor.

If this model would be true, one would expect that Hrp1 is still bound to cleavage-defective mRNAs. To investigate the binding of Hrp1 to its specific targets, we carried out RIP experiments with Hrp1 in wild-type and *cft2-1* cells grown at 30°C. As expected, we found an ∼2-fold increased binding of Hrp1 to its mRNA targets, indicating that these RNAs remain bound to Hrp1 for a longer time until the faulty transcript is degraded (Figure 5D, E). In comparison, Hrp1 bound to the unspecific rRNA targets *ETS1* and *ITS1* to a similar level as to the no tag control in both the wild type and *cft2-1*, supporting its function as a specific mRNA quality control factor as no specific binding was identified for the rRNA (Figure 5F). Interestingly, and in contrast to Hrp1, when we performed a similar RIP experiment with Rna14, we found an over ∼50% decrease in its association with the target mRNAs (Figure 5G, H), supporting a model in which Rna14 binding to Hrp1 might be the trigger of the Mex67 recruitment and suggesting Rna14 to function as an indicator of correct cleavage. To finally address whether Rna14 is not only absent from the pre-mRNAs but also from the CPF–CF complex itself, we carried out co-IPs with two different proteins of the CPF–CF complex, Cft1 and Pfs2. We found that while the interaction between these proteins and Rna14 was detectable in wild-type cells, it was significantly reduced in *cft2-1* mutants (Figure 5I, J; Supplementary Fig. S3E, F). These findings suggest that Rna14 potentially associates at a final step of the termination reaction. Importantly, it reveals that Rna14 must be associated with the complex for Hrp1 to recruit Mex67.

Taken together, our data identify Hrp1 as a novel guard protein that monitors the CPF–CF-mediated 3′ cleavage of pre-mRNAs. It is recruited to the EE, located at the 3′ end of the transcript. Upon correct formation of the CPF–CF complex and the contact of Hrp1 with Rna14, Hrp1 recruits the export receptor Mex67 for nuclear export of the correctly matured mRNA (Figure 6). In case defects in the CPF—CF-mediated cleavage occur, transcription continues until the next termination site. Fail-safe termination by the NNS complex results in the recruitment of the TRAMP complex and the exosome for degradation of the faulty transcript. Its nuclear export is prevented through the presence of Hrp1, which in the absence of Rna14 cannot bind Mex67 and then functions as a retention factor, as the absence of Mex67 from Hrp1 is detected by Mlp1 at the NPC, and transfer to the cytoplasm is prevented. The absence of Hrp1 results in the loss of the nuclear 3′ end cleavage surveillance and in the leakage of elongated faulty transcripts into the cytoplasm.

DISCUSSION

Originally, Hrp1 was identified as a suppressor of temperature-sensitive mutants of *NPL3* (34). Its domain structure is very similar to that of Npl3 and the other guard proteins Gbp2 and Hrb1 (Figure 1B). Like Npl3, it contains two RRMs and an SR/RGG domain at its C-terminus. Interestingly, it not only has structural similarities, but also shows functional analogies to these guard proteins. It is, for example, loaded onto the pre-mRNA in the nucleus and shuttles with the mRNA into the cytoplasm (25,48). This is unique for a protein of the CPF–CF complex, but similar to the guard proteins. Additionally, we were able to show that Hrp1 can act as a retention factor for mRNAs. In high copy, it visibly retains mRNAs in the nucleus, which leads to growth defects (Figure 1C, D). This is likewise similar to the other guard proteins. Furthermore, *HRP1* genetically interacts with mutants of *MEX67* and *MLP1* (Figure 1G). These combined mutations are problematic because the coupling of a defective 3′ end quality control with impaired mRNA export or poor NPC surveillance is not tolerable. Additionally, Hrp1 physically interacts with the export receptor heterodimer Mex67–Mtr2 and the NPC gatekeeper Mlp1 (Figure 1E, F, H; Supplementary Fig. S1D). The coverage of the guard proteins with Mex67 is necessary to relieve the nuclear retention of the mRNA, and the Mex67 coverage is controlled by Mlp1 at the NPC (3,8,49). Although so many similarities exist between all guard proteins, there is one interesting difference between Hrp1 and the other guards. While all guards show interactions with the degradation machinery (2,5,16), we cannot confirm this for Hrp1. However, this might not be necessary for this specific guard, because prevention of 3′ cleavage usually automatically leads to a downstream-located NNS fail-safe site via which the TRAMP complex and subsequently the exosome is recruited to eliminate this RNA (50,51).

One of the two functions that has been reported for Hrp1 is the participation in NMD (35). This is interesting because the other guard proteins have not only nuclear but also cytoplasmic surveillance functions. The splicing guard proteins Gbp2 and Hrb1 also support NMD (18), where they repress translation and support the degradation of the faulty mRNA. Npl3 remains bound to the mRNA until it is translated by the ribosome (52), and is also required for ribosomal subunit joining and thus efficient translation in

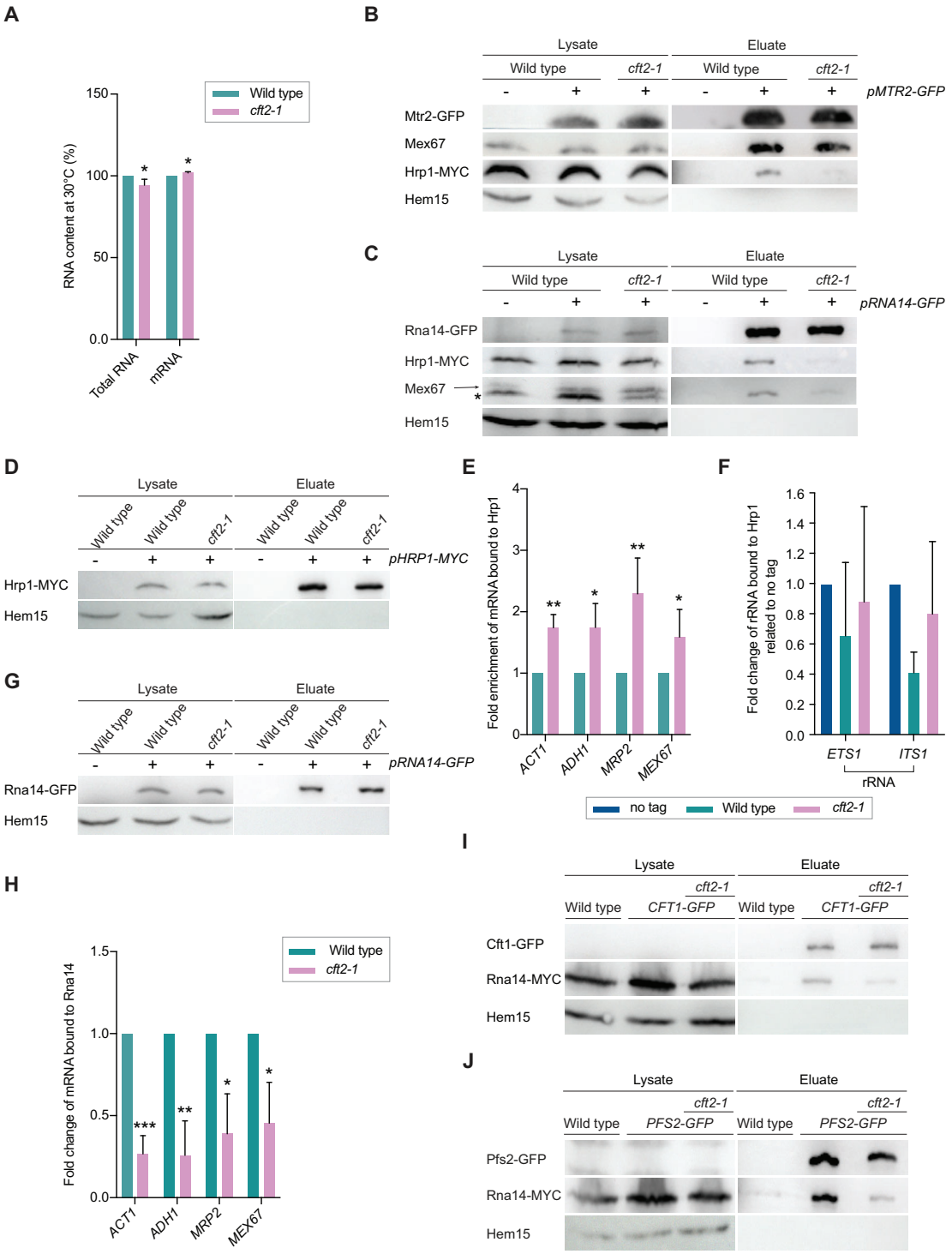

Figure 5. The contact of Hrp1 with Rna14 represents a switch towards nuclear mRNA export. (**A**) mRNA generated in *cft2-1* grown at 30°C is stable. Equal amounts of cell pellets were harvested after reaching the logarithmic growth phase. The total RNA was isolated and measured at OD_{260}. Equal amounts of total RNA were further purified and the mRNA content was determined; $n = 4$. (**B**) The contact of Mex67–Mtr2 with Hrp1 is impaired in the termination-defective mutant *cft2-1*. A western blot of the Mtr2–GFP-co-precipitated Mex67 and the MYC-tagged Hrp1 is shown in wild-type and *cft2-1* cells; $n = 4$. (C) Rna14 does not interact with Hrp1 and Mex67 in termination-defective cells. A western blot of co-precipitated Hrp1 and Mex67 with Rna14 is shown from wild-type and *cft2-1* cells. The asterisk indicates a band that is a result of a cross-reaction with the MYC antibody; $n = 5$. (**D**) An example western blot of the Hrp1 pulldown used in (E) is shown. Hem15 served as a negative control. (**E** and **F**) Defects in transcription termination result in an increased association of Hrp1 with its target mRNAs (E) but not with unspecific rRNAs (F). The RNA for the RIP experiment was isolated and used in subsequent qPCRs; $n = 5$. (**G**) An example western blot of the Rna14 pulldown used in (H) is shown. (**H**) Defects in transcription termination result in a decreased precipitation of Hrp1 target mRNAs with Rna14. The RNA for the RIP experiment was isolated and used in subsequent qPCRs; $n \geq 4$. (**I** and **J**) Rna14 is not incorporated into the CPF–CF complex in *cft2-1*. Western blots of co-immunoprecipitated Rna14-MYC with GFP-tagged Cft1 or Pfs2 are shown. All strains used in this figure were cultivated at 30°C before harvest and lysis. Hem15 served as a negative control; $n = 3$.

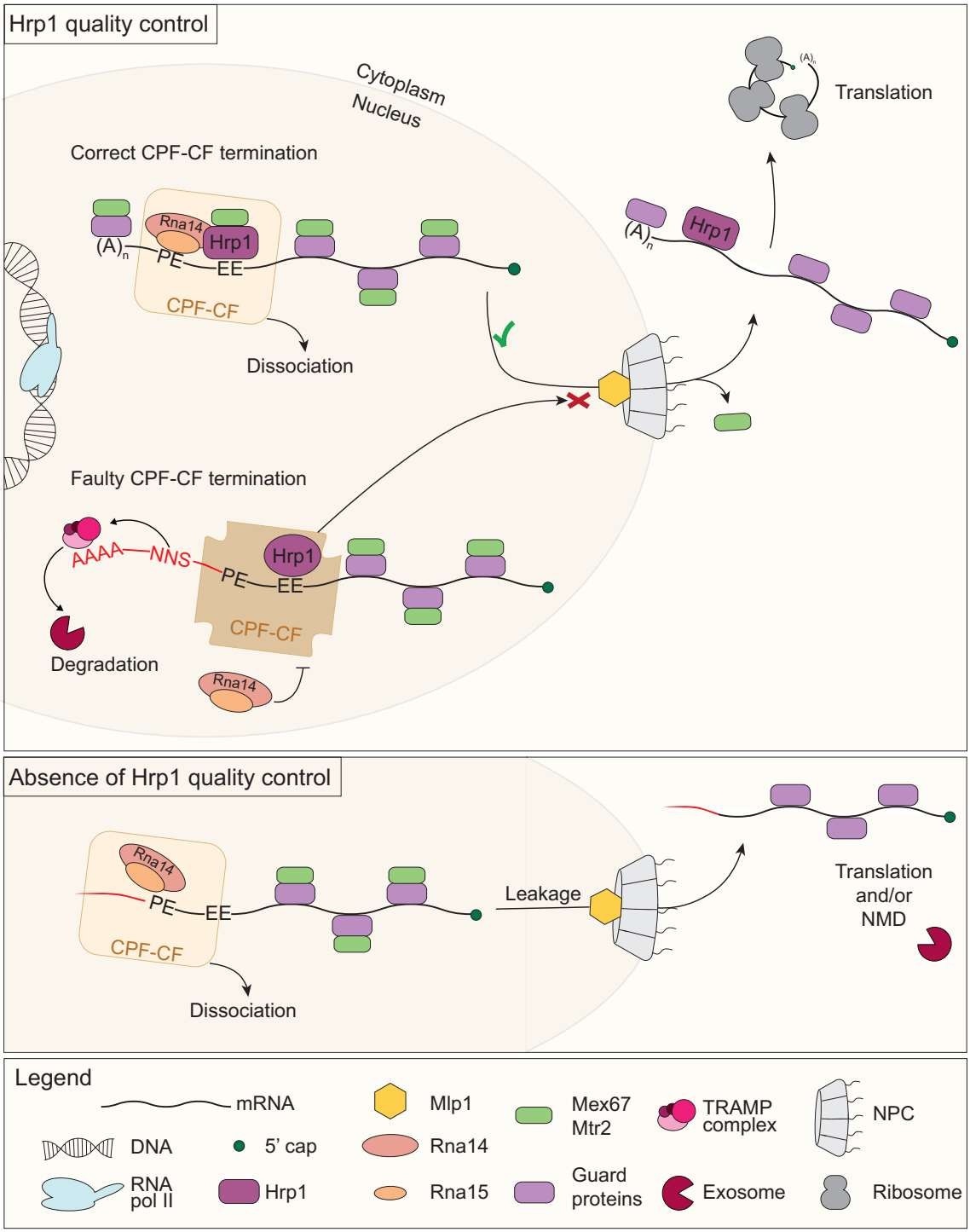

Figure 6. Model for the role of Hrp1 as a guard protein that monitors pre-mRNA 3′ cleavage. Top: intact Hrp1 quality control. If the CPF–CF complex is properly assembled and the pre-mRNA is correctly cleaved, Hrp1 recruits the export receptor Mex67–Mtr2 upon contact with Rna14. Mex67–Mtr2 coverage of the mRNA via Hrp1, and also the other guard proteins that monitor other maturation steps, promotes mRNA export through the NPC for subsequent translation. In case the cleavage complex does not assemble properly, as for instance in *cft2-1*, Rna14 cannot bind. In this situation, Hrp1 detects the missing protein and is unable to bind Mex67 for mRNA export. As a consequence, the faulty transcript is retained, which results from recognition of the uncovered Hrp1 by the surveillance gate keeper Mlp1 at the NPC. Subsequently, readthrough mRNAs are captured by the NNS complex, marked with a short poly(A) tail by the TRAMP complex and degraded by the exosome. Bottom: absence of Hrp1 quality control. When Hrp1 is missing, elongated mRNAs are not retained and can leak into the cytoplasm because the other guard proteins exhibit Mex67 coverage.

the cytoplasm (53). Taking these published data and our new experimental discoveries into account, the findings illustrate striking similarities of Hrp1 to the other guard proteins in surveillance of mRNAs from their emergence in the nucleus until their translation in the cytoplasm.

Besides its cytosolic function in NMD, a second function for Hrp1 has been reported for the 3′-end processing of pre-mRNAs in the nucleus. There, it seems to assist in the cleavage site selection rather than in the RNA scission, as cleavage is still feasible in its absence, but occurs at multiple sites (32,54). Sequence recognition of the EE occurs via the two RRMs in Hrp1 (55). The PE is recognized through an RRM in Rna15, but only when it is in association with Hrp1 (56,57). Their interaction is mediated through the scaffolding protein Rna14 (27,58). This function of Hrp1 in helping to stabilize the whole CPF–CF complex on the correct termination site can already be interpreted as a quality control function that supports the production of correctly cleaved transcripts. Nevertheless, we found an additional surveillance function by preventing the export of elongated transcripts (Figures 3E and 4F). Furthermore, Hrp1 is special compared with the other factors of the CPF–CF complex because its mutation or deletion does not lead to an mRNA accumulation in the nucleus, in contrast to mutations in *RNA14*, *RNA15*, *PCF11* and *CLP1*, which result in the visible accumulation of mRNAs in the nucleus (33,59,60) (Figure 3E). As a quality control factor, Hrp1 rather retains mRNA upon overexpression (Figure 1C, D). Its absence leads to the opposite phenotype: mRNA leakage into the cytoplasm (Figures 3D, E and 4F–K). The accumulation of mRNAs in the other CPF–CF mutants, in contrast, reflects that defective mRNAs are generated and prevented from being exported into the cytoplasm. Interestingly, a few elongated mRNAs are also produced naturally in wild-type cells and in mutants of *HRP1* (Figure 4B), but their nuclear retention is abrogated in the absence of intact Hrp1 (Figures 2G and 4F–K). Remarkably, we saw a downstream shift of transcript ends and detected an ∼2-fold increase of the elongated transcripts in the cytoplasm of *hrp1-1* which is influenced by >60% of all expressed transcripts (Figure 4I–L). This large number of elongated transcripts that were detected in the cytoplasm of *hrp1-1* (Figure 4K) shows that Hrp1 is required for the majority of the CPF–CF-terminated transcripts, which reflects its prominent role in quality control of the cleavage reaction. It furthermore suggests that Hrp1 is a 3′ end quality control factor that can actively retain elongated transcripts in the nucleus. The 3′-elongated mRNAs that have failed the CPF–CF cleavage are terminated at downstream-situated NNS-binding sites. This leads to the immediate degradation of the faulty RNAs, as the NNS system is coupled to the TRAMP- and exosome-mediated degradation of the transcripts (44–46).

When comparing the yeast and the mammalian transcription termination mechanisms, some differences are evident. While the yeast CPF–CF complex and the mammalian cleavage and polyadenylation specificity factor (CPSF)–CF complex show high similarities, the yeast NNS complex as such has not been identified in mammals (44,61). Rather, an altered CPSF–CF complex in association with the CBC and ARS2 channels transcripts into degradation by the nuclear exosome targeting (NEXT) complex and thus shows a conserved principle for the degradation of unwanted transcript (44). Interestingly, senataxin, the Sen1 homolog in human cells, has been shown to be involved in mRNA termination, indicating that it has a conserved function in unwinding and dissociating transcripts from transcription sites (62). The export of matured transcripts in mammals relies on the export receptor TAP–p15, which is highly homologous to Mex67–Mtr2 in yeast. TAP also interacts with serine/arginine-rich (SR) proteins, that are homologs to the guard proteins Npl3, Gbp2 and Hrb1. Like the yeast guard proteins, some of the human SR proteins shuttle in association with TAP–p15 to the cytoplasm and some of them have been shown to interact with the nuclear RNA degradation machinery (4,63). It seems likely that these proteins are also involved in the quality control of the 3′ end maturation.

Why are these elongated pre-mRNAs generally undesirable for a cell? First, transcription of downstream-located genes can be affected by the readthrough or interference of the generation and degradation of cryptic unstable transcripts (CUTs). Transcription into the next open reading frame reduces the production of this gene, which might affect cell viability. Interference with the generation of CUTs might also alter gene expression (44). In yeast, the transcription units are closer together than in mammalian cells, which might necessitate tighter termination control (44,61). However, also in human cells, transcriptional readthrough has been shown to result in the production of RNA chimeras, which are frequently detected in cancer cells (64).

A second reason why elongated transcripts can be harmful to cells is that the elongated mRNAs themselves are most probably less efficiently translated, (i) because on a longer RNA it takes the ribosomes longer to circle on the transcript and (ii) mRNAs with long 3′-untranslated regions are more prone to be degraded by NMD, which ultimately reduces the amount of the gene product (65). Thus, the efficient and immediate elimination of RNAs that cannot be terminated by the CPF–CF system is an important part of the surveillance and mRNA quality assurance mechanisms in cells.

To date, many reports describe the negative impact of deficient polyadenylation in Mammalia, but knowledge on the effects of cleavage site readthrough is widely missing. Interestingly, a correlation between an increased transcription readthrough and a lower survival rate of human cancer patients exists (64). In particular, transcriptional readthrough and the altered expression of the *BCL2* oncogene was described for kidney cancer (clear cell renal cell carcinoma, ccRCC) (64). Therefore, our study is an important step towards understanding the quality control of eukaryotic transcription termination. Identifying CF IB/Hrp1 as the 3′ end quality control factor in yeast fills a gap in the knowledge of the stepwise and complete surveillance of the mRNA maturation process.

DATA AVAILABILITY

All data are stored at the Gesellschaft für wissenschaftliche Datenverarbeitung mbH Göttingen (GWDG). Sequencing data from cytoplasmic fractionation have been uploaded

to the NCBI Gene Expression Omnibus (GEO; www.ncbi.nlm.nih.gov/geo/) with the accession number GSE231488.

SUPPLEMENTARY DATA

Supplementary Data are available at NAR Online.

ACKNOWLEDGEMENTS

We are grateful to C. Gonzalez, U. Mühlenhoff and D. Tollervey for providing plasmids, strains or antibodies.
Author contributions: Experiments were designed and data interpreted by J.L., L.Q. and H.K.; all experiments were carried out by J.L. except those in Figures 1G–I, 2E–G, 3A, 3C, 3E, 4B–E, 4H, 5E, 5F, 5H, and 5J, and Supplementary Figures S1A–D, S2A, S2C, S3A–C, and S3A and S3F which were done either by L.Q. or by both J.L and L.Q. together. RNA-sequencing was conducted by G.S., and analysis of the data shown in Figure 4I–L by I.C. The manuscript was written by H.K.; all authors discussed the results and commented on the manuscript.

FUNDING

The University of Göttingen based on DFG funding [SFB860 and KR 1779/12-1 to H.K.]; the China Scholarship Council (CSC) [to J.L.].
Conflict of interest statement. The authors declare that they have no conflict of interest.

REFERENCES

1. Meinel,D.M. and Sträßer,K. (2015) Co-transcriptional mRNP formation is coordinated within a molecular mRNP packaging station in *S. cerevisiae*. *Bioessays*, **37**, 666–677.
2. Hackmann,A., Wu,H., Schneider,U.M., Meyer,K., Jung,K. and Krebber,H. (2014) Quality control of spliced mRNAs requires the shuttling SR proteins Gbp2 and Hrb1. *Nat. Commun.*, **5**, 3123.
3. Zander,G., Hackmann,A., Bender,L., Becker,D., Lingner,T., Salinas,G. and Krebber,H. (2016) mRNA quality control is bypassed for immediate export of stress-responsive transcripts. *Nature*, **540**, 593–596.
4. Zander,G. and Krebber,H. (2017) Quick or quality? How mRNA escapes nuclear quality control during stress. *RNA Biol*, **14**, 1642–1648.
5. Vanácová,S., Wolf,J., Martin,G., Blank,D., Dettwiler,S., Friedlein,A., Langen,H., Keith,G. and Keller,W. (2005) A new yeast poly(A) polymerase complex involved in RNA quality control. *PLoS Biol.*, **3**, e189.
6. Hurt,E., Sträßer,K., Segref,A., Bailer,S., Schlaich,N., Presutti,C., Tollervey,D. and Jansen,R. (2000) Mex67p mediates nuclear export of a variety of RNA polymerase II transcripts. *J. Biol. Chem.*, **275**, 8361–8368.
7. Green,D.M., Johnson,C.P., Hagan,H. and Corbett,A.H. (2003) The C-terminal domain of myosin-like protein 1 (Mlp1p) is a docking site for heterogeneous nuclear ribonucleoproteins that are required for mRNA export. *Proc. Natl Acad. Sci. USA*, **100**, 1010–1015.
8. Soheilypour,M. and Mofrad,M.R.K. (2018) Quality control of mRNAs at the entry of the nuclear pore: cooperation in a complex molecular system. *Nucleus*, **9**, 202–211.
9. Lykke-Andersen,S. and Jensen,T.H. (2015) Nonsense-mediated mRNA decay: an intricate machinery that shapes transcriptomes. *Nat. Rev. Mol. Cell Biol.*, **16**, 665–677.
10. Mitchell,P. and Tollervey,D. (2000) Musing on the structural organization of the exosome complex. *Nat. Struct. Biol.*, **7**, 843–846.
11. Fox,M.J. and Mosley,A.L. (2016) Rrp6: integrated roles in nuclear RNA metabolism and transcription termination. *Wiley Interdiscip. Rev. RNA*, **7**, 91–104.
12. Sloan,K.E., Schneider,C. and Watkins,N.J. (2012) Comparison of the yeast and human nuclear exosome complexes. *Biochem. Soc. Trans.*, **40**, 850–855.
13. Tutucci,E. and Stutz,F. (2011) Keeping mRNPs in check during assembly and nuclear export. *Nat. Rev. Mol. Cell Biol.*, **12**, 377–384.
14. Callahan,K.P. and Butler,J.S. (2010) TRAMP complex enhances RNA degradation by the nuclear exosome component Rrp6. *J. Biol. Chem.*, **285**, 3540–3547.
15. Doma,M.K. and Parker,R. (2007) RNA quality control in eukaryotes. *Cell*, **131**, 660–668.
16. Klama,S., Hirsch,A.G., Schneider,U.M., Zander,G., Seel,A. and Krebber,H. (2022) A guard protein mediated quality control mechanism monitors 5′-capping of pre-mRNAs. *Nucleic Acids Res.*, **50**, 11301–11314.
17. Kress,T.L., Krogan,N.J. and Guthrie,C. (2008) A single SR-like protein, Npl3, promotes pre-mRNA splicing in budding yeast. *Mol. Cell*, **32**, 727–734.
18. Grosse,S., Lu,Y.Y., Coban,I., Neumann,B. and Krebber,H. (2021) Nuclear SR-protein mediated mRNA quality control is continued in cytoplasmic nonsense-mediated decay. *RNA Biol.*, **18**, 1390–1407.
19. Baejen,C., Torkler,P., Gressel,S., Essig,K., Söding,J. and Cramer,P. (2014) Transcriptome maps of mRNP biogenesis factors define pre-mRNA recognition. *Mol. Cell*, **55**, 745–757.
20. Schmid,M., Olszewski,P., Pelechano,V., Gupta,I., Steinmetz,L.M. and Jensen,T.H. (2015) The nuclear polyA-binding protein Nab2p is essential for mRNA production. *Cell Rep.*, **12**, 128–139.
21. Graber,J.H., McAllister,G.D. and Smith,T.F. (2002) Probabilistic prediction of *Saccharomyces cerevisiae* mRNA 3′-processing sites. *Nucleic Acids Res.*, **30**, 1851–1858.
22. Guo,Z., Russo,P., Yun,D.F., Butler,J.S. and Sherman,F. (1995) Redundant 3′ end-forming signals for the yeast CYC1 mRNA. *Proc. Natl Acad. Sci. USA*, **92**, 4211–4214.
23. Casanal,A., Kumar,A., Hill,C.H., Easter,A.D., Emsley,P., Degliesposti,G., Gordiyenko,Y., Santhanam,B., Wolf,J., Wiederhold,K. *et al.* (2017) Architecture of eukaryotic mRNA 3′-end processing machinery. *Science*, **358**, 1056–1059.
24. Amrani,N., Minet,M., Le Gouar,M., Lacroute,F. and Wyers,F. (1997) Yeast Pab1 interacts with Rna15 and participates in the control of the poly(A) tail length in vitro. *Mol. Cell. Biol.*, **17**, 3694–3701.
25. Kessler,M.M., Henry,M.F., Shen,E., Zhao,J., Gross,S., Silver,P.A. and Moore,C.L. (1997) Hrp1, a sequence-specific RNA-binding protein that shuttles between the nucleus and the cytoplasm, is required for mRNA 3′-end formation in yeast. *Genes Dev.*, **11**, 2545–2556.
26. Kessler,M.M., Zhao,J. and Moore,C.L. (1996) Purification of the *Saccharomyces cerevisiae* cleavage/polyadenylation factor I. Separation into two components that are required for both cleavage and polyadenylation of mRNA 3′ ends. *J. Biol. Chem.*, **271**, 27167–27175.
27. Minvielle-Sebastia,L., Preker,P.J. and Keller,W. (1994) RNA14 and RNA15 proteins as components of a yeast pre-mRNA 3′-end processing factor. *Science*, **266**, 1702–1705.
28. Takagaki,Y. and Manley,J.L. (1997) RNA recognition by the human polyadenylation factor CstF. *Mol. Cell. Biol.*, **17**, 3907–3914.
29. Mandel,C.R., Bai,Y. and Tong,L. (2008) Protein factors in pre-mRNA 3′-end processing. *Cell. Mol. Life Sci.*, **65**, 1099–1122.
30. Gross,S. and Moore,C.L. (2001) Rna15 interaction with the A-rich yeast polyadenylation signal is an essential step in mRNA 3′-end formation. *Mol. Cell. Biol.*, **21**, 8045–8055.
31. Dichtl,B. and Keller,W. (2001) Recognition of polyadenylation sites in yeast pre-mRNAs by cleavage and polyadenylation factor. *EMBO J.*, **20**, 3197–3209.
32. Minvielle-Sebastia,L., Beyer,K., Krecic,A.M., Hector,R.E., Swanson,M.S. and Keller,W. (1998) Control of cleavage site selection during mRNA 3′ end formation by a yeast hnRNP. *EMBO J.*, **17**, 7454–7468.
33. Hammell,C.M., Gross,S., Zenklusen,D., Heath,C.V., Stutz,F., Moore,C. and Cole,C.N. (2002) Coupling of termination, 3′ processing, and mRNA export. *Mol. Cell. Biol.*, **22**, 6441–6457.
34. Henry,M., Borland,C.Z., Bossie,M. and Silver,P.A. (1996) Potential RNA binding proteins in *Saccharomyces cerevisiae* identified as suppressors of temperature-sensitive mutations in NPL3. *Genetics*, **142**, 103–115.
35. Gonzalez,C.I., Ruiz-Echevarria,M.J., Vasudevan,S., Henry,M.F. and Peltz,S.W. (2000) The yeast hnRNP-like protein Hrp1/Nab4 marks a

transcript for nonsense-mediated mRNA decay. *Mol. Cell*, **5**, 489–499.
36. Gibson,D.G., Young,L., Chuang,R.-Y., Venter,J.C., Hutchison,C.A. and Smith,H.O.(2009) Enzymatic assembly of DNA molecules up to several hundred kilobases. *Nat. Methods*, **6**, 343–345.
37. Gietz,D., St Jean,A., Woods,R.A. and Schiestl,R.H. (1992) Improved method for high efficiency transformation of intact yeast cells. *Nucleic Acids Res.*, **20**, 1425.
38. Beißel,C., Neumann,B., Uhse,S., Hampe,I., Karki,P. and Krebber,H. (2019) Translation termination depends on the sequential ribosomal entry of eRF1 and eRF3. *Nucleic Acids Res.*, **47**, 4798–4813.
39. Shukla,S. and Parker,R. (2014) Quality control of assembly-defective U1 snRNAs by decapping and 5′-to-3′ exonucleolytic digestion. *Proc. Natl Acad. Sci. USA*, **111**, E3277–E3286.
40. Kim,D., Langmead,B. and Salzberg,S.L. (2015) HISAT: a fast spliced aligner with low memory requirements. *Nat. Methods*, **12**, 357–360.
41. Ramírez,F., Ryan,D.P., Grüning,B., Bhardwaj,V., Kilpert,F., Richter,A.S., Heyne,S., Dündar,F. and Manke,T. (2016) deepTools2: a next generation web server for deep-sequencing data analysis. *Nucleic Acids Res.*, **44**, W160–W165.
42. Tudek,A., Schmid,M., Makaras,M., Barrass,J.D., Beggs,J.D. and Jensen,T.H. (2018) A nuclear export block triggers the decay of newly synthesized polyadenylated RNA. *Cell Rep.*, **24**, 2457–2467.
43. Tuck,A.C. and Tollervey,D. (2013) A transcriptome-wide atlas of RNP composition reveals diverse classes of mRNAs and lncRNAs. *Cell*, **154**, 996–1009.
44. Porrua,O. and Libri,D. (2015) Transcription termination and the control of the transcriptome: why, where and how to stop. *Nat. Rev. Mol. Cell Biol.*, **16**, 190–202.
45. Singh,P., Chaudhuri,A., Banerjea,M., Marathe,N. and Das,B. (2021) Nrd1p identifies aberrant and natural exosomal target messages during the nuclear mRNA surveillance in *Saccharomyces cerevisiae*. *Nucleic Acids Res.*, **49**, 11512–11536.
46. Rondon,A.G., Mischo,H.E., Kawauchi,J. and Proudfoot,N.J. (2009) Fail-safe transcriptional termination for protein-coding genes in *S. cerevisiae*. *Mol. Cell*, **36**, 88–98.
47. Kyburz,A., Sadowski,M., Dichtl,B. and Keller,W. (2003) The role of the yeast cleavage and polyadenylation factor subunit Ydh1p/Cft2p in pre-mRNA 3′-end formation. *Nucleic Acids Res.*, **31**, 3936–3945.
48. Henry,M.F. and Silver,P.A. (1996) A novel methyltransferase (Hmt1p) modifies poly(A)+-RNA-binding proteins. *Mol. Cell. Biol.*, **16**, 3668–3678.
49. Zander,G., Kramer,W., Seel,A. and Krebber,H. (2017) *Saccharomyces cerevisiae* Gle2/Rae1 is involved in septin organization, essential for cell cycle progression. *Yeast*, **34**, 459–470.
50. Vasiljeva,L. and Buratowski,S. (2006) Nrd1 interacts with the nuclear exosome for 3′ processing of RNA polymerase II transcripts. *Mol. Cell*, **21**, 239–248.
51. LaCava,J., Houseley,J., Saveanu,C., Petfalski,E., Thompson,E., Jacquier,A. and Tollervey,D. (2005) RNA degradation by the exosome is promoted by a nuclear polyadenylation complex. *Cell*, **121**, 713–724.
52. Windgassen,M., Sturm,D., Cajigas,I.J., Gonzalez,C.I., Seedorf,M., Bastians,H. and Krebber,H. (2004) Yeast shuttling SR proteins Npl3p, Gbp2p, and Hrb1p are part of the translating mRNPs, and Npl3p can function as a translational repressor. *Mol. Cell. Biol.*, **24**, 10479–10491.
53. Baierlein,C., Hackmann,A., Gross,T., Henker,L., Hinz,F. and Krebber,H. (2013) Monosome formation during translation initiation requires the serine/arginine-rich protein Npl3. *Mol. Cell. Biol.*, **33**, 4811–4823.
54. Hill,C.H., Boreikaite,V., Kumar,A., Casanal,A., Kubik,P., Degliesposti,G., Maslen,S., Mariani,A., von Loeffelholz,O., Girbig,M. *et al.* (2019) Activation of the endonuclease that defines mRNA 3′ ends requires incorporation into an 8-subunit core cleavage and polyadenylation factor complex. *Mol. Cell*, **73**, 1217–1231.
55. Perez-Canadillas,J.M. (2006) Grabbing the message: structural basis of mRNA 3′UTR recognition by Hrp1. *EMBO J.*, **25**, 3167–3178.
56. Barnwal,R.P., Lee,S.D., Moore,C. and Varani,G. (2012) Structural and biochemical analysis of the assembly and function of the yeast pre-mRNA 3′ end processing complex CF I. *Proc. Natl Acad. Sci. USA*, **109**, 21342–21347.
57. Qu,X., Perez-Canadillas,J.M., Agrawal,S., De Baecke,J., Cheng,H., Varani,G. and Moore,C. (2007) The C-terminal domains of vertebrate CstF-64 and its yeast orthologue Rna15 form a new structure critical for mRNA 3′-end processing. *J. Biol. Chem.*, **282**, 2101–2115.
58. Noble,C.G., Walker,P.A., Calder,L.J. and Taylor,I.A. (2004) Rna14–Rna15 assembly mediates the RNA-binding capability of *Saccharomyces cerevisiae* cleavage factor IA. *Nucleic Acids Res.*, **32**, 3364–3375.
59. Carneiro,T., Carvalho,C., Braga,J., Rino,J., Milligan,L., Tollervey,D. and Carmo-Fonseca,M. (2008) Inactivation of cleavage factor I components Rna14p and Rna15p induces sequestration of small nucleolar ribonucleoproteins at discrete sites in the nucleus. *Mol. Biol. Cell*, **19**, 1499–1508.
60. Brodsky,A.S. and Silver,P.A. (2000) Pre-mRNA processing factors are required for nuclear export. *RNA*, **6**, 1737–1749.
61. Eaton,J.D. and West,S. (2020) Termination of transcription by RNA polymerase II: BOOM!. *Trends Genet.*, **36**, 664–675.
62. Skourti-Stathaki,K., Proudfoot,N.J. and Gromak,N. (2011) Human senataxin resolves RNA/DNA hybrids formed at transcriptional pause sites to promote Xrn2-dependent termination. *Mol. Cell*, **42**, 794–805.
63. Huang,Y., Gattoni,R., Stevenin,J. and Steitz,J.A. (2003) SR splicing factors serve as adapter proteins for TAP-dependent mRNA export. *Mol. Cell*, **11**, 837–843.
64. Grosso,A.R., Leite,A.P., Carvalho,S., Matos,M.R., Martins,F.B., Vitor,A.C., Desterro,J.M., Carmo-Fonseca,M. and de Almeida,S.F. (2015) Pervasive transcription read-through promotes aberrant expression of oncogenes and RNA chimeras in renal carcinoma. *Elife*, **4**, e09214.
65. Kebaara,B.W. and Atkin,A.L. (2009) Long 3′-UTRs target wild-type mRNAs for nonsense-mediated mRNA decay in *Saccharomyces cerevisiae*. *Nucleic Acids Res.*, **37**, 2771–2778.